



HAL
open science

Big Earth data processing using machine learning for integrated mapping of the Dead Sea Fault, Jordan

Polina Lemenkova

► **To cite this version:**

Polina Lemenkova. Big Earth data processing using machine learning for integrated mapping of the Dead Sea Fault, Jordan. *Glasnik Šumarskog fakulteta Univerziteta u Banjoj Luci*, 2021, 31, pp.79-103. 10.7251/GSF2131079L . hal-03505790

HAL Id: hal-03505790

<https://hal.science/hal-03505790>

Submitted on 31 Dec 2021

HAL is a multi-disciplinary open access archive for the deposit and dissemination of scientific research documents, whether they are published or not. The documents may come from teaching and research institutions in France or abroad, or from public or private research centers.

L'archive ouverte pluridisciplinaire **HAL**, est destinée au dépôt et à la diffusion de documents scientifiques de niveau recherche, publiés ou non, émanant des établissements d'enseignement et de recherche français ou étrangers, des laboratoires publics ou privés.



Distributed under a Creative Commons Attribution 4.0 International License

BIG EARTH DATA PROCESSING USING MACHINE LEARNING FOR INTEGRATED MAPPING OF THE DEAD SEA FAULT, JORDAN

OBRADA “BIG EARTH DATA” PODATAKA KORIŠĆENJEM MAŠINSKOG UČENJA ZA INTEGRISANO MAPIRANJE NA PRIMJERU RASJEDA MRTVOG MORA U JORDANU

Polina Lemenkova^{1*}

¹ Université Libre de Bruxelles. École polytechnique de Bruxelles (Brussels Faculty of Engineering), Laboratory of Image Synthesis and Analysis (LISA). Building L, Campus de Solbosch, Avenue Franklin Roosevelt 50, Brussels 1000, Belgium
ORCID ID: <https://orcid.org/0000-0002-5759-1089>

*e-mail: polina.lemenkova@ulb.be; pauline.lemenkova@gmail.com

Abstract

In this research, an integrated framework on the big Earth data analysis has been developed in the context of the geomorphology of Jordan. The research explores the correlation between several thematic datasets, including machine learning and multidisciplinary geospatial data. GIS mapping is widely used in geological mapping as the most adequate technical tool for data visualization and analysis. GIS applications encourage geological prospective modeling by visualizing data aimed at the prognosis of mineral resources. However, automatization using machine learning for big Earth data processing provides the speed and accurate processing of multisource massive datasets. This is enabled by the application of scripting and programming in cartographic techniques. This study presents the combined machine learning methods of cartographic analysis and big Earth data modeling. The objective is to analyze a correlation between the factors affecting the geomorphological shape of Jordan with respects to the Dead Sea Fault and geological evolution. The technical methodology includes the following three independent tools: 1) Generic Mapping Tools (GMT); 2) Selected libraries of R programming language; 3) QGIS. Specifically, the GMT scripting program was used for topographic, seismic and geophysical mapping, while QGIS was used for geologic mapping and R language for geomorphometric modeling. Accordingly, the workflow is logically structured through these three technical tools, representing different cartographic approaches for data processing. Data and materials include multisource datasets of the various resolution, spatial extent, origin and formats. The results presented cartographic layouts of qualitative and quantitative maps with statistical summaries (histograms). The novelty of this approach is explained by the need to close a technical gap between the traditional GIS and scripting mapping, which is wider for big data mapping and where the crucial factors are speed and precision of data handling, as well as effective visualization achieved by the machine graphics. The paper analyzes the underlying geologic processes affecting the formation of geomorphological landforms in Jordan with a 3D visualization of the selected fragment of the Dead Sea Fault zone. The research presents an extended description in methodology, including the explanations of code snippets from the GMT modules and examples of the use of R libraries *'raster'* and *'tmap'*. The results revealed strong correlation between the geological and geophysical settings which affect geomorphological patterns. Integrated study of the geomorphology of Jordan was based on multisource datasets processed by scripting. A thorough analysis presented regional correlations between the geomorphological, geological and tectonic settings in Jordan. The paper contributed both to the development of cartographic engineering by introducing scripting techniques and to the regional studies of Jordan including the Dead Sea Fault as a special region of Jordan. The results include 12 new thematic maps including a 3D model.

Keywords: big data, cartography, Dead Sea Fault, geology, geophysics, GMT, Jordan, machine learning, QGIS, topography

1. INTRODUCTION / UVOD

1.1 Theoretical framework / Teorijski okvir

From the development of geoinformatics since the 1990s, the use of Geographical Information Systems (GIS) as a cartographic concept has been referred to as an optimal technical tool in geospatial data modeling in the engineering cartography and CAD domains. GIS has become a well-developed method of mapping and modeling through a convincing pool of research papers (Farhan et al., 2013, 2016; Govedar & Bilić, 2020) and there is a widely reported use of various GIS, e.g. ArcGIS, SAGA GIS, ERDAS Imagine, QGIS, ILWIS GIS and other software in geologic engineering (Kuhn et al., 2006; Alnawafleh et al., 2013; Abed, 2018; Čomić & Anikić, 2020), hazard and risk mapping (Al-Sheriadeh et al., 2000; Lemenkova et al., 2012; Halilović et al., 2020).

GIS applications in forestry are diverse due to the excellent capabilities of GIS to visualize the

spatial data, perform vegetation analysis, e.g. using remote sensing Landsat TM/ETM+ data, as reflected in various applications and previous studies (e.g. Foody & Hill 1996; Salvador & Pons, 1998; Miletić et al. 2016; Valjarević et al., 2018a). However, the use of GUI-based software has certain limitations compared to the scripting-based approach. In addition, technical cartographic applications of the integrated use of programming languages parallel to GIS are not still well established in the existing cartographic engineering literature. For example, by contrast to numerous uses of GIS (Petković et al. 2015; Stupar & Milanović, 2017; Marder et al., 2018) or visualizing stratigraphic lithologic columns in geologic engineering (Abed & Yaghan, 2000; Khrewesh et al., 2014), the research literature related to the use of shell scripting in cartography and applications of R language is rather limited (Lemenkova, 2019a; 2019b).

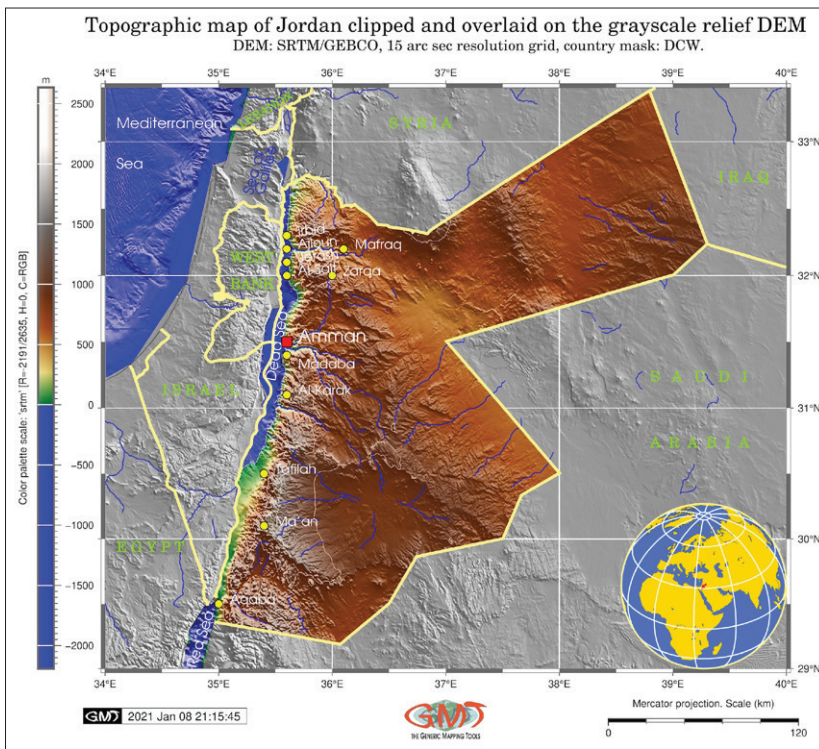


Figure 1. Topographic map of Jordan / **Slika 1.** Topografska karta Jordana (Source / Izvor: GEBCO clipped and overlaid over the SRTM DEM)

Though there are some publications on plotting by R and Generic Mapping Tools (GMT) scripting in a cartographic domain (e.g. Lemenkova, 2020a, 2020b), the literature on the integrated use of GIS with programming languages linked to the geomorphological modeling and geological data visualization is scarce. Furthermore, the cartographic workflow is typically discussed in unspecific terms referring to the general methodology of the visualization process, e.g. using functions of vector analysis and statistics, spatial queries, overlay and interpolation, image processing, general questions of terrain analy-

sis, data conversion, reprojecting, clipping and subsetting.

At the same time, there is a knowledge-generating side of geoinformatics connected to the creation of qualitative aspects of data in geological engineering. Being a quantitative-oriented technical tool for data modeling, cartography gradually included both qualitative and quantitative data processing which opened the new perspectives of integrated data analysis in mineral resource prospecting (Sadooni & Dalqamouni, 1998).



Figure 2. Google Earth aerial perspective image of Jordan / **Slika 2.** Google Earth vazdušna perspektiva Jordana (Source / Izvor: Google Earth Pro, DCW)

This significantly improved the existing fundamental literature on geologic engineering of Jordan (see e.g. Quennell, 1951; Burdon, 1959; Bender, 1968, 1974a, 1974b; Eyal & Reches, 1983) through the improved data analysis, modeling and visualization. Advanced Google Earth technology today enables the visualization of the Earth's surface and features of interest thereon in more detail and accuracy based on the aerial images (Figure 2).

The objective of this study is to address the issues of cartographic scripting framework in the

region of Jordan (Figure 1) through qualitative data visualization using scripting solutions of GMT, Quantum GIS (QGIS), and libraries of R programming language. The study is focused on the integration of geologic, geophysical, tectonic and lithological factors influencing the geomorphology of Jordan.

The novelty of this research is the automatization in the mapping of Jordan, which has been achieved by the combined scripting cartographic approach using GMT and R with the additional use of QGIS. The automated machine learning

approach for topographic, geomorphological and geophysical mapping of Jordan contrasts with the existing use of the traditional GIS.

Innovativeness is also contained in the presented simple use of the open multisource datasets combined from various free repositories and presented by the aerial imagery (Google Earth), geophysical and topographic raster grids, geological vector layers, tabular data for seismic earthquake mapping and textual description on Jordan natural setting (geology, topography, geophysical, geomorphological and tectonics). Management of such diverse data and materials required the technical approaches integrated into a project which was demonstrated and explained with notes in corresponding sections of the manuscript.

1.2 Motivation and aims / Motiv i ciljevi

The abovementioned perspective of digital cartographic engineering tools relates not only to the technically improved data visualization, represented by the print high-quality maps using GMT and fine graphical plotting by R or Python. Another important feature of the advanced cartographic technical approaches in geologic engineering is data integration which includes database generation and database application. Thus, it enables the accumulation of various big data containing information on geomorphology, geology, tectonics, seismicity, topography, bathymetry, geophysics and geodesy for visualization and performing correlation analyses between these data with the final aim of geological analysis, modeling and prognosis.

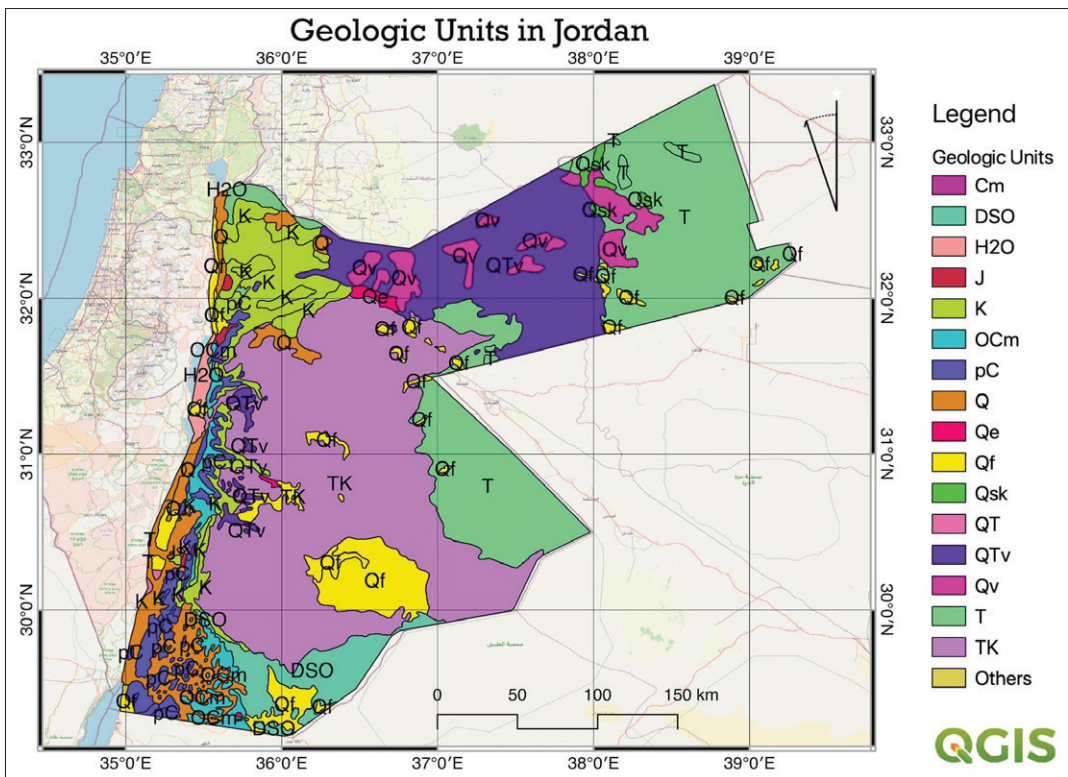


Figure 3. Geologic units in Jordan / Slika 3. Geološke jedinice u Jordanu (Source / Izvor: USGS, OpenStreet-Maps)

This paper adopts an integrated application of the console-based GMT scripting toolset with

R programming language (using RStudio environment) and a menu-based QGIS. The func-

tionality of scripting modules, the diversity of QGIS plugins integrating the Google Earth, Open StreetMaps datasets for mapping the USGS geological data (Figure 3), and the extended data processing in R cartographic packages are considered as potentially leading to

the improved cartographic data visualization, engineering, data modeling and analysis by the application of diverse tools for various formats (raster NetCDF GRD and IMG formats, vector *.shp* files, tabular *.txt*, *.gmt*, *.ngdc* and *.csv* formats).

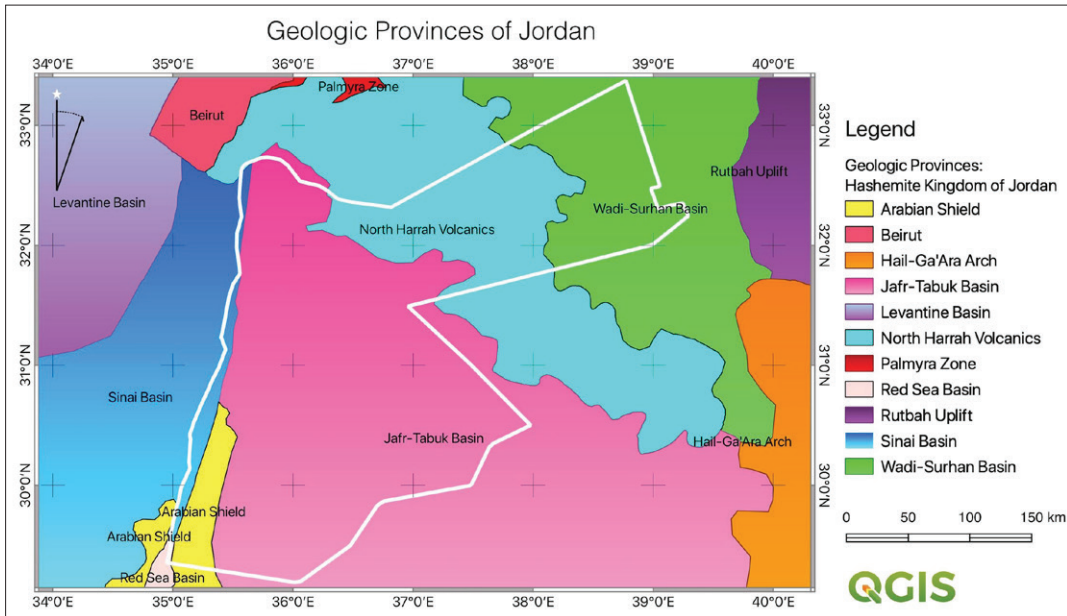


Figure 4. Geologic provinces in and around Jordan / **Slika 4.** Geološke provincije u Jordanu i oko njega (Source / Izvor: USGS)

An integrated cartographic framework has been developed to perform a complex geomorphological analysis of Jordan, including its geology, topography, geophysical settings, and 3D visualization of the Dead Sea Fault, modeled using high-resolution datasets from publicly available geospatial repositories. Analyzing the existing cartographic engineering methods, the most suitable and comprehensive approach for a complex geomorphological and geological mapping is the integrated approach that processes large datasets by technical tools flexibly interchanged for different workflows: GMT for 2D topographic, geophysical and seismic mapping, *'grdview'* module for 3D mapping, R for a geomorphological model of the terrain analysis by combination of *'raster'* and *'tmap'* packages, QGIS for geological and lithological mapping (Figure 3 and Figure 4).

Taking into account the diversity of the relief in Jordan, which was largely controlled by the tectonic history and geologic evolution of the region (Amireh et al., 1994), the variations in local and regional settings are discussed in the following section based on the extensive review of the relevant existing literature on the geology and topography of Jordan. An R language was used for geomorphological modeling using the DEM dataset and a combination of *'raster'* and *'tmap'* libraries. Namely, it was applied for exploring selected geomorphometric parameters of Jordan (slope, aspect, and hillshade) to show the relationship between the actual relief and geologic driving forces affecting its formation.

2. MATERIALS AND METHODS / MATERIJAL I METODE

The methodology presents an integrated cartographic scripting approach aimed at the analysis of the geomorphology of Jordan with a special focus on the Dead Sea Fault in the context of geological formation and evolution. Technical mapping tools include three software: GMT, QGIS, and R. The GMT is a scripting cartographic toolset developed in 1991 (Wessel et al., 2019). The QGIS (QGIS.org, 2020) has been used for geological mapping. The geologic and lithologic vector layers were imported into QGIS version 3.16 (Hannover) and organized in the project with selected layers handled using the Processing Toolbox of the QGIS. The QGIS was selected for geological data processing since it is compatible with the ArcGIS shape format. ArcGIS is widely used in GIS mapping (Valjarević, 2018b; Lemenkova, 2020f). The functionality of the QGIS is achieved by a variety of plugins, flexible integration with Python, GRASS GIS and SAGA GIS, compatibility with ArcGIS, and free open-source availability. Modeling the relief of Jordan has been performed using libraries of R language (R Core Team, 2020) used by RStudio (RStudio Team, 2017).

2.1 Data collection and integration / Prikupljanje i integracija podataka

Datasets were collected from the open-source repositories. Quantitative spatial high-resolution data have been visualized and modeled using GMT, QGIS, and R. One dataset was collected from a topographic GEBCO grid (Schenke, 2016; GEBCO Compilation Group, 2020) based on the SRTM (Becker et al., 2009; Tozer et al., 2019) and ETOPO1 (Amante & Eakins, 2009). The resolution is based on a technical approach of quantitative data processing (Smith & Sandwell, 2003): 15 arc second for GEBCO (Figure 1 and Figure 8) and 1 arc minute for ETOPO1 (Figure 5). GEBCO, SRTM, and ETOPO1 data are widely used in geospatial visualization and engineering (Dill et al., 2012; Drăguț & Eisank, 2012; Oruç et al., 2019; Lemenkova, 2020c, 2020d) due to the exceptionally high quality and reliability which ensures the most comprehensive view of the Earth's topography.

The aerial imagery data were obtained through the Google Earth service (Figure 2) linking the topographic relief view of the Earth with Jordan's borders by the Digital Chart of the World (DCW), the most comprehensive GIS global database of the Earth. The advantage of satellite imagery in geospatial engineering (Lemenkova, 2011, 2014; Löhrer et al., 2013; Riad et al., 2020) consists of the possibilities of integrated data visualization.

Besides visualizing and reflecting the actual shape of the Earth, the remote sensing data provide information that can be combined in a more complex way to study correlations of different factors affecting the geologic structure and topographic relief of the Earth. The most well-known remote sensing data include Sentinel-1A/2A satellite images (e.g. Fiaschi et al., 2017; Lemenkova, 2020e), SPOT (Klinger et al., 2000b), and the Landsat TM (Ginat et al., 1998; Al Hseinat et al., 2020). This study uses Google Earth aerial image for a perspective view of the topography of Jordan.

The data on earthquakes (Figure 8) were collected from the IRIS (Incorporated Research Institution for Seismology) database catalog (1974 to 2020), using the coordinate extent of Jordan captured as a search parameter. The earthquakes are shown based on two parameters, the magnitude and depth (from -1 to -33 km). The geologic data (Figure 3 and 4) were obtained from the opensources of the United States Geological Survey (USGS) as a dataset containing vector files in 'shp' format (Pollastro et al. 1999).

The geophysical datasets include the geoid model of the Earth EGM-2008 (Pavlis et al., 2012) and the gravity free-air Faye's anomaly (Sandwell et al., 2014) obtained from the numerical grids in NetCDF format (Figure 6 and Figure 7). The gravity data have a high accuracy and quality, improved resolution, and coverage of the marine gravity field, as described in relevant papers (Sandwell & McAdoo, 1990; Sandwell et al., 2013).

The input data for geomorphological modeling consisted of Digital Elevation Models (DEM) at a standard 30 m (SRTM DEM 30) resolution for terrain analysis and variables (slope, aspect, hillshade) to quantify a geomorphological setting in Jordan. Specifically, the relief modeling of slope (Figure 9), aspect (Figure 10), hillshade (Figure 11) and elevation (Figure 12) have been performed by the DEM acquired from the University of California, Davis as a dataset in R package ‘*raster*’ (Hijmans & van Etten, 2012). The geomorphological models by R were screened visually for map output and updated using ‘*tmap*’ package thereafter.

2.2 GMT scripting / GMT skripte

The workflow in GMT was carried out as specified by the scripting methodology, using several modules for the graphical processing of raster grids. Figure 1 shows the topographic map of the country made using the overlay techniques for the clipping region of Jordan selected by the DCW over the monochrome image of the surrounding region. The main GMT modules used for mapping include the following workflow as below:

- a. The ‘*grdcut*’ module was used for selecting the study area: ‘*gmt grdcut GEBCO_2019.nc-R34/40/29/34 -Gjo_relief.nc*’
- b. The ‘*makecpt*’ module was used for creating the color palette according to the topographic range: ‘*gmt makecpt -Csrtm.cpt -T-2191/2635 -A50 > jordan.cpt*’
- c. The ‘*pscoast*’ modules were used to create a mask of the vector layer from DCW of the country’s polygon: ‘*gmt pscoast -R34/40/29/33.5 -JM6.5i -Dh -M -EJO > jordan.txt*’
- d. The ‘*grdimage*’ module was used for the visualization of a raster grid: ‘*gmt grdimage jo_relief.nc -Cjordan.cpt -R34/40/29/33.4 -JM6.5i -I+a15+ne0.75 -Xc -P -K > \$ps*’
- e. The Unix ‘*echo*’ utility was used to generate the topography image with shading: ‘*echo “-10000 150 10000 150” > gray.cpt*’
- f. The ‘*psclip*’ module was used to clip the map by the DCW layer to only include Jordan: ‘*gmt psclip -JM -R jordan.txt -O -K >> \$ps*’
- g. The ‘*pstext*’ module was used for annotating the cities: ‘*gmt pstext -R -J -N -O -K -F+f12p,13,white+jLB >> \$ps << EOF 35.7 31.5 Amman EOF*’
- h. The ‘*psxy*’ module was used for adding the cities using coordinates: ‘*gmt psxy -R -J -Ss -W0.5p -Gred -O -K << EOF >> \$ps 35.6 31.5 0.35c EOF*’
- i. The ‘*logo*’ module was used to add the GMT logo: ‘*gmt logo -Dx7.0/-2.0+o0.1i/0.1i+w2c -O -K >> \$ps*’
- j. The ‘*grdcontour*’ module was used to add topographic isolines (plotted every 500 m): ‘*gmt grdcontour jo_relief1.nc -R -J -C500 -Wthinnest,dimgrey -O -K >> \$ps*’

The demonstrated scripting technology has been applied for plotting maps shown in Figure 1, 6, 7, and 8. Spatial distribution modeling of the earthquakes in Jordan (Figure 8) has been performed by the GMT module ‘*psxy*’ with the database of IRIS for the period 1974–2020 as the event data with magnitude and depth of the foci, to analyze the epicenters of the earthquakes. The data visualization has been performed by following the code: ‘*gmt psxy -R -J quakes_Jordan.gmt -Wfaint -i4,3,6,6s0.1 -h3 -Scc -Csteps.cpt -O -K >> \$ps*’ where the visualized points show the magnitude of the events using the available method (Lemenkova, 2021).

The 3D mesh model of the Dead Sea Fault shown in Figure 5 was visualized using the ‘*grdview*’ module by the following code: ‘*gmt grdview jo_relief5.nc -J -R -JZ3.5c -Cmyrelief.cpt -p205/30 -Qsm -N-3500+glightgray -Wm0.07p -Wf0.1p,red -B4/4/2000:”Bathymetry and topography (m)”:-ESwZ -S5 -Y5.0c -O -K >> \$ps*’ following the methodology of the GMT with its syntax.’

2.3 QGIS mapping / Kartiranje u QGIS-u

The QGIS has been applied for geologic and lithologic mapping. Geological mapping plays an essential role in the analysis of the relief in such a tectonically active area as Jordan in general and the Dead Sea Fault in particular. The Dead Sea

Fault presents a particular landform of Jordan with a clear asymmetry in structure and a rift-like morphology along its southern part (Smit et al., 2010). The geomorphology of the Dead Sea Fault region mirrors the variability of land elevations at both global and regional scales. In this way, it reflects the intensity of the exogenic and inner factors affecting local and regional variability of relief. The *'Vector Overlay'* operation of the Processing Toolbox in the QGIS was used as a tool for clipping the area of Jordan using the mask of DCW. The layers were organized using the *'Layer Manager'* and adjusted by the categorized color palettes. The maps (Figure 3 and Figure 4) were prepared using the *'Layout Manager'* of QGIS.

2.4 R programming / Programiranje u R-u

Geomorphometric modeling aimed at geomorphological analysis (Figures 9, 10, 11 and 12) was performed using a set of packages (libraries) of R language and operated by an RStudio environment: *'sp'*, *'raster'*, *'ncdf4'*, *'RColorBrewer'*, *'sf'* and *'tmap'*. The libraries *'raster'* and *'tmap'* are the most important use for relief modeling and cartographic plotting, respectively.

The DEMs of Jordan were imported into R by *'raster'* package and analyzed using the *'terrain'* function tool, as described below in more technical details. The *'ncdf4'* package was applied for the processing of the data formats. Accordingly, the *'RColorBrewer'* package was used for color visualization. The auxiliary packages *'sp'* and *'sf'* were used for operating with classes and methods for spatial data and processing simple features, which is a standard way to encode spatial vector data by R.

3. REZULTATI / RESULTS

3.1 Topographic modeling by high-resolution datasets / Topografsko modeliranje pomoću podataka visoke rezolucije

The resulting maps are presented in Figure 9–12 showing various aspects of the geomorphometric parameters in the relief of Jordan with expla-

The *'raster'* package of R is a stand-alone geographical library and data processing package that was developed especially for geomorphometry applications, such as slope and aspect analysis, DEM and hillshade visualization. The *'tmap'* package of R is a cartographic package that was developed specifically for the mapping and visualization of geoinformation. The workflow in R includes the following steps:

- i. Data capture by the *'getData'* function of *'raster'*: `'alt = getData("alt", country = "Jordan", path = tempdir())'`
- ii. Modeling slope, aspect and, hillshade by *'raster'* package of R: `'slope = terrain(alt, opt = "slope")'`. `'aspect = terrain(alt, opt = "aspect")'`. `'hill = hillShade(slope, aspect, angle = 40, direction = 270)'`
- iii. Visualizing the DEM and the resulting plots (aspect, slope, and hillshade): `plot(alt)`
- iv. Mapping by *'tmap'* package using the *'plot'* mode: `'tmap_mode("plot")'`.
- v. Selecting the suitable color `'tmaptools::palette_explorer()'`
- vi. Mapping by using the scheme for the maps in Figure 9 – 12: `'map1 <- tmap_style() + tm_shape(slope, title = 'Slope') + tm_raster() + tm_scale_bar() + tm_compass(type = "radar") + tm_layout()'`. The additional refinements (font types, sizes, location of the cartographic elements, colors, rotation of ticks, several levels of annotations (title, subtitle, panel title, legend, etc.) were adjusted using these functions by R syntax.
- vii. Visualizing maps: `'map1'`
- viii. Saving graphical output as a JPG file: `'tmap_save(map1, "Jordan_Slope.jpg", dpi = 300, height = 10)'`

nations presented in the Results section. Based on the results, a strong relationship between the structural geologic setting and terrain complexity (roughness, steepness, and curvature) was evident, thus providing a strong quantitative correlation performed by using the script-

ing framework techniques between geological, topographic, and geomorphological settings in Jordan. Figure 1 and Figure 2 show the topography of Jordan compared to the other countries. Its topography consists mainly of a plateau with a dominating range between 700 to 1,200 m and the whole study area has a range of -2,191 m to 2,635m (according to the GEBCO dataset as found by 'gdalinfo' utility of GDAL).

The topography of Jordan is mostly divided into a series of ridges by valleys, gorges, wadis, and a few mountainous areas. The dominating part of the eastern region of Jordan (East Bank) is covered by desert, with mainly arid geomorphic landforms (Abu-Allaban et al., 2015): sands, dunes, salt flats, low mountains, located especially in the south and southeast (Abed, 1982, 2000).

The range of the topography values observed is comparable to the distribution of the most notable major topographic features in Jordan: Wadi Mujib located at the 31,4°N 35,5°E, a river canyon entering the Dead Sea from the east, Wadi Araba (Jarar et al., 1983; Atallah, 1992; Klinger et al., 1997), Wadi Shueib catchment area (Obeidat et al., 2021), a basin of the Yarmouk River, which is the largest tributary of the Jordan River on its south (Obeidat et al., 2013), Wadi Mujib (Abed, 2017), the depression of the Araba valley, situated between the Dead Sea Fault and the Gulf of Aqaba covered by alluvial and lacustrine deposits (Klinger et al., 2000a).

3.2 Spatial distribution of geologic units and provinces by data overlay / Geografska distribucija geoloških jedinica i provincija

According to the performed mapping, Tertiary Cretaceous (TK) outcrops across the Cretaceous-Tertiary boundary are evident for the major territory of the country (purple color in Figure 3). Among others, Figure 3 visualizes the following geologic units of Jordan: Tertiary (Paleogene and Neogene) outcrops which are mostly located in the north-eastern and eastern regions of the country (green color in Figure 3).

Earlier units from the Tertiary and Cretaceous period (TK in the map) occupy the dominant

areas in the center of the country (lilac colors in Figure 3). Accordingly, the outcrops on other geologic units are presented by the Cambrian (Cm), Devonian Silurian Ordovician (DSO), Jurassic (J), Ordovician Cambrian (OCm), Precambrian undifferentiated (pC) and Quaternary (Q). Quaternary is subdivided subsequently into the Quaternary fluvial (Qf), Quaternary eolian (Qe), Quaternary sahbka (Qsk), Quaternary Tertiary (QT), Quaternary volcanic (Qv) and Quaternary Tertiary volcanic (Qtv) considering the geomorphological landforms.

Comparing Figure 3 with Figure 4 shows that Cambrian (Precambrian undifferentiated (pC), dark lilac color in Figure 3) to Devonian (Devonian Silurian Ordovician (DSO), light green color in Figure 3), Quaternary (Q, brown color in Figure 3) non-marine clastic sedimentary rocks are located along the edge of the Arabian Shield (yellow color in Figure 4, southern Jordan). These were deposited prior to the breakup of the eastern platform into a set of the northward oriented horsts and grabens during the Hercynian Orogeny, as also pointed in previous studies (Al-Laboun, 1986).

3.3 Spatial extent of notable geologic provinces

/ Prostorni opseg značajnih geoloških provincija

The visualized dominant geologic province distribution of an area (Figure 4) provides new data on the regional geologic patterns for their relationship between the major geologic elements, geophysical fields, topography, and geomorphology of Jordan. Cartographic mapping of the provinces includes several blocks. The Jafr-Tabuk Basin Province is shown as a dominating part (bright magenta), which is important since this region is a source of oil shale source rocks. The region has a total organic carbon content exceeding 3% and mixed oil/gas-prone to oil-prone potential (Alsharhan & Nairn, 1997).

The formation of the North Harrat Volcanics (bright cyan color in Figure 4) is located along the Harrat al-Sham region of the rocky, basaltic desert (Edgell, 2006), which further extends to southern Syria, Jordan, and the northern Arabian Peninsula. This area has been geologically

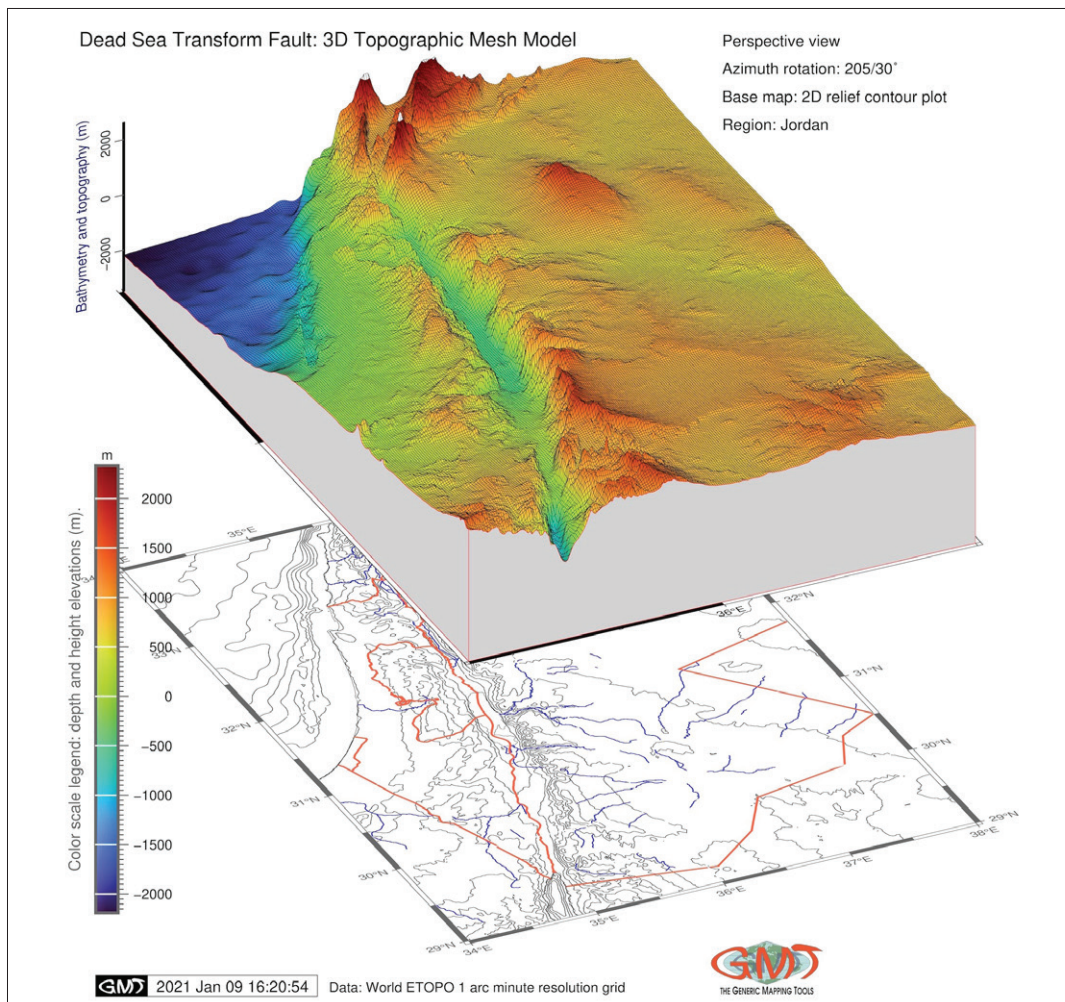


Figure 5. 3D model of the Dead Sea Fault / **Slika 5.** 3D model rasjeda Mrtvog mora (Source / Izvor: Data: ETOPO1)

formed by the tectonic activity from the Oligocene through Quaternary (Al Kwatli et al., 2015). Geologically, it is known for over 800 volcanic cones and 140 dikes, which makes it the largest among the existing several volcanic fields on the Arabian Plate (Krienitz et al., 2007).

The Wadi Sirhan, a wide depression, was attributed to the NW-SE-trending (colored bright green in Figure 4) which shows relatively large, extended sandy, marshy lowland. The spatial distribution of the area well correlates with the location of the Triassic geologic units (compare Figure 4 with Figure 3 where this area (T) is represented by bright

green color). The outcrops of Quaternary volcanic (Qv, magenta) well correlate with the distribution of the NE borders of the North Harrah Volcanics. Other geological units are annotated on the map (Hail-Ga'Ara Arch, Rutbah Uplift, Beirut, Levantine Basin, Sinai Basin).

3.4 Three-dimensional mesh modelling of the topographic grid / Modeliranje topografske mreže korišćenjem 3D mesh-a

Three-dimensional (3D) modeling is an important technique used widely in Earth sciences. 3D-modeling provides an effective visualization of surfaces based on the coordinate triples in

space (Fialko et al., 2005; Barbot et al., 2009; Lemenkov & Lemenkova, 2021). In this study, the 3D model demonstrates a perspective visualization of the most notable topographic depression of Jordan: the Dead Sea Fault (Figure

5). The Dead Sea Fault is a part of the Great Rift Valley, a remarkable geologic object, stretching in an NS direction from Lebanon to Mozambique, and consisting of several continuous rifts and trenches of varying sizes and elevations.

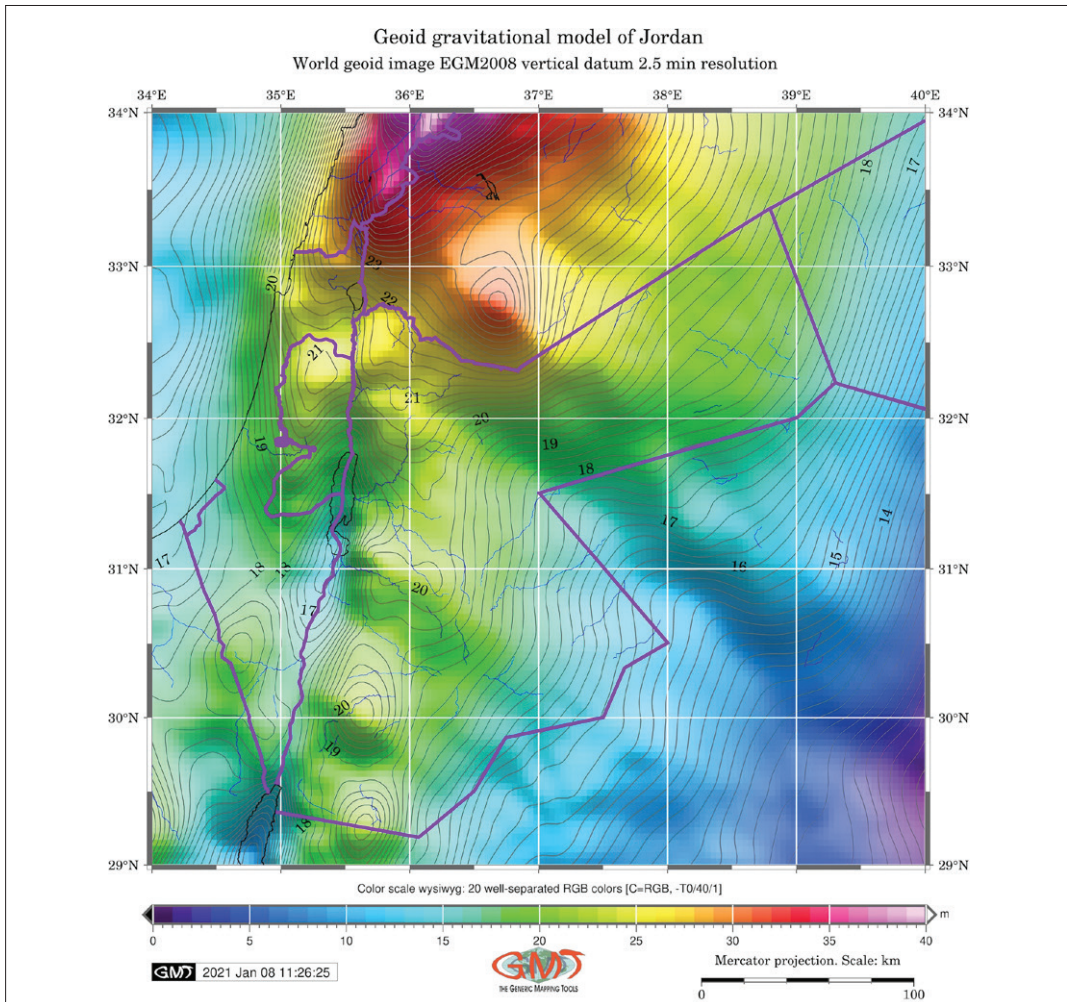


Figure 6. Geoid gravitational model of Jordan / **Slika 6.** Geoidni gravitacioni model Jordana (Source / Izvor : EGM-2008)

The Dead Sea Fault is an important part of the world geologic and geodynamic formations. In its origin, it is deeply connected to the geodynamic processes and movement of the two tectonic plates: Arabian and African. The Dead Sea Fault presents a transform plate boundary, along which these two plates slide past one another. As the 3D transect traversed the Dead Sea Fault

zone, the visualized mesh grid from the ETOPO1 was utilized as a measure of roughness as the GMT method well presented the curvature of the surface using 3D visualization technique over the 2D relief contour map. The presented 3D model shows the Dead Sea fault zone, a major left-lateral strike-slip fault extending over cca. 160 km to the Gulf of Aqaba (Klinger et al., 2000a). The

3D modeling represents a sound approach to the perspective mapping of data applied in various papers related to geological modeling (Abu Rajab & Al Tarazi, 2018; Lemenkova, 2019d).

In contrast to the existing GIS techniques for 3D modeling, the GMT provides a novel, scripting method based on the 'grdview' model to quantify the surface using mesh elements in a raster grid on a user-defined resolution scale of the 3D model. The 3D modeling numerically simulates the structure of the relief and geomorphology of the varied landforms within the selected enlarged study area within the coordinates 34°/38° E, 29°/34° N in the southern Jordan and the Dead Sea Fault zone.

3.5 Geophysical fields modeled by GMT / Modelovanje geofizičkih polja pomoću GMT-a

The geophysical data, along with datasets on surface geology, drilling, seismic reflection, are the key source of information for the Dead Sea basin structure (Garfunkel & Ben-Avraham, 1996) since they contain information on the physical setting of the Earth's surface and subsurface. The geophysical facilitate the analysis and prognosis on the location of hydrocarbons, oil plays and minerals, aggregate and mineral resources. Two datasets were modeled in the part of geophysical modeling in this research: the gravity fields and the geoid.

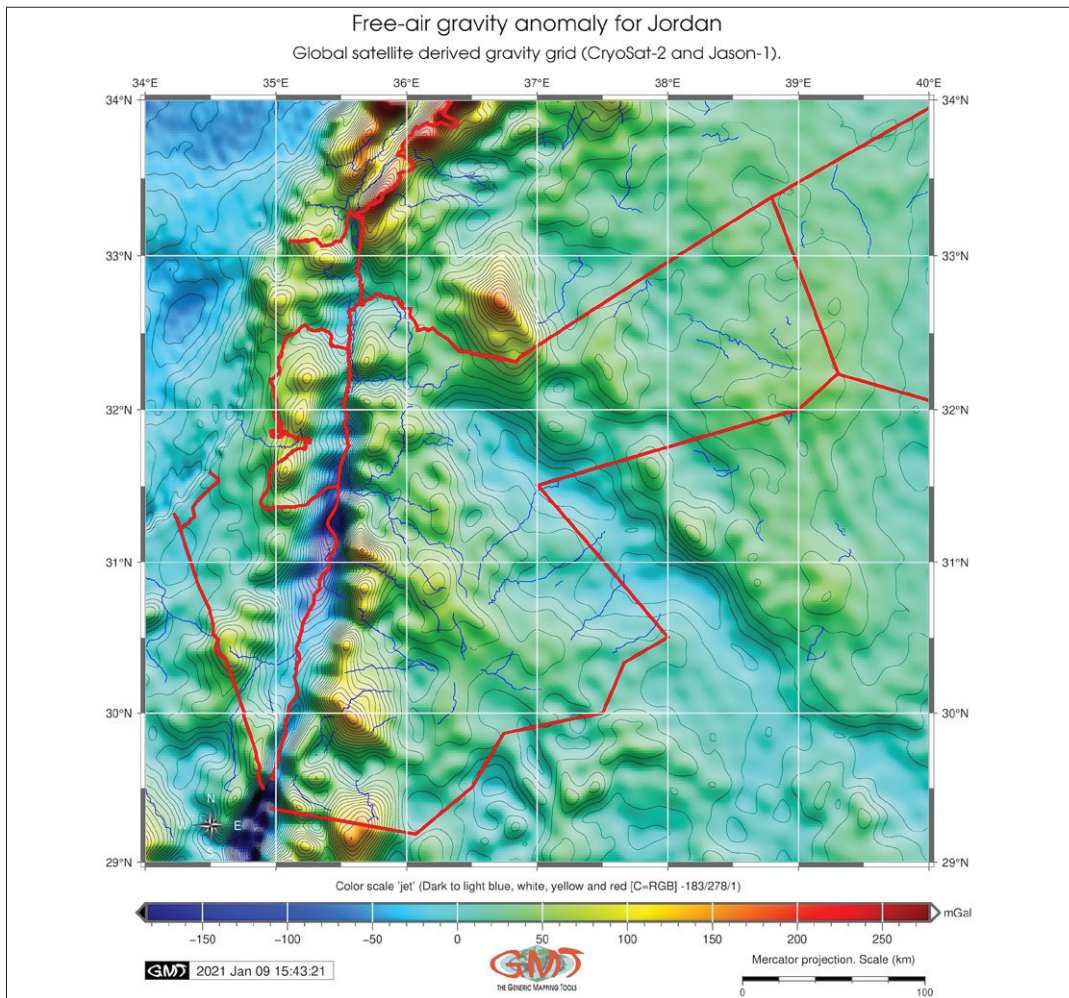


Figure 7. Free-air gravity anomaly map of Jordan / **Slika 7.** Mapa anomalije gravitacije slobodnog vazduha Jordana (Source / Izvor: Data: gravity CryoSat-2 and Jason-1)

3.5.1 Geoid model / Model geoida

Figure 6 presents the model of geoid made using the EGM-2008 grid. The geoid undulation shows the geodetic measurements of the Earth's heights in terms of gravity showing the shape that the Earth's surface would have taken under the influence of the gravity and rotation of the Earth alone (Fowler, 2005; Sideris, 2011). The relationship between geoid height and topography shows the compensation of

the Earth's surface for the effects of gravity in a non-linear complex function (Marks & Sandwell, 1991). The geoid shows generally higher values on the region northward of the country (the region of modern Syria) with the detected values between 35 to 40 m (bright pink color in Figure 6), while the lowest values are mostly located in the SE region of Jordan (0 to 5 m in geoid undulations), colored in dim blue to dark purple in Figure 6.

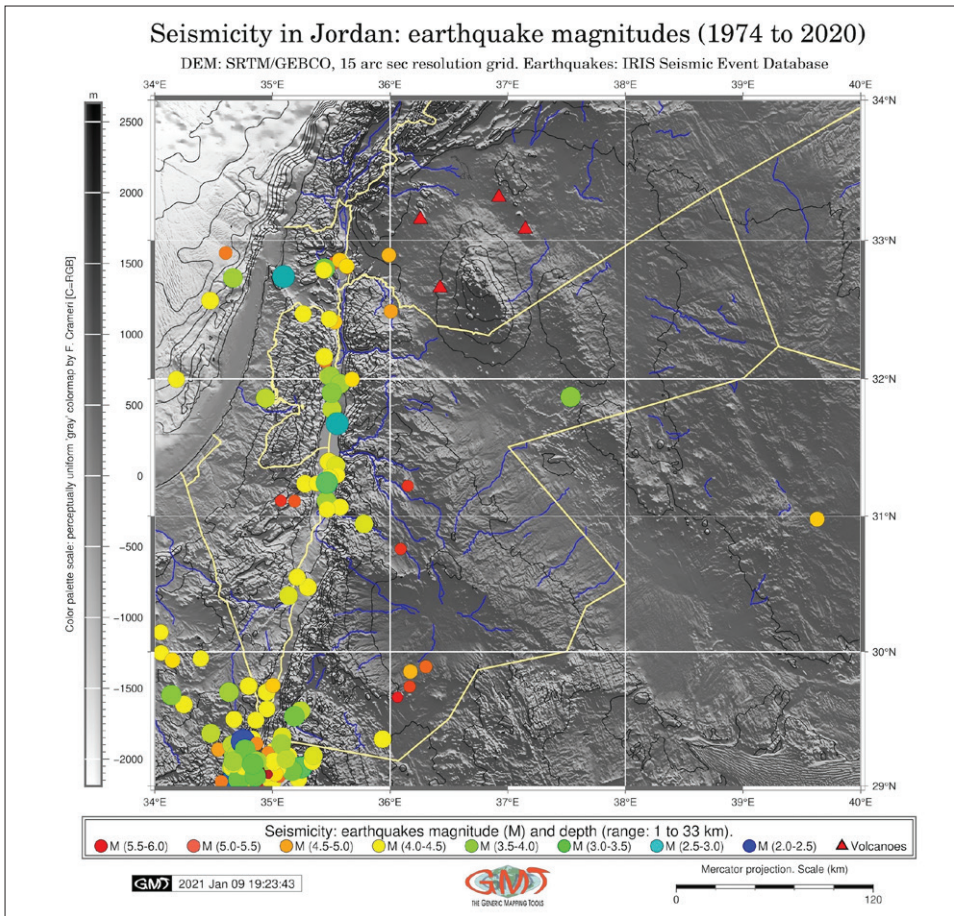


Figure 8. Seismicity in Jordan (1974–2020) / **Slika 8.** Seizmičnost u Jordanu (1974–2020)
(Source / Izvor: IRIS, GEBCO)

The variability of the geoid heights correlates with the rock properties depending on the proportion of porosity and the values of density and reflecting variations in the mantle of the Earth. Other effects on the geoid from the tectonics

are shown in the previous research (Sandwell & Schubert, 1980) where the geoid height/age relations are illustrated using the data from Geos 3 altimeter showing a positive correlation of geoid with a spreading velocity.

3.5.2 Free-air gravity model / Model gravitacije

Gravity anomalies represent variations in density and rock masses distributed unequally over the Earth. Anomalies in gravity depend on various parameters. The consistency between the topography and gravity measurement results showed a correlation between the parameters such as topographic depth, gravity values, and geographic location (in general, sea-level gravity increases from the Equator to the poles due to the equatorial bulge and the effects of the Earth's rotation). Other parameters include lithospheric density, elastic and mechanical thicknesses of the lithosphere and geophysical measurements: flexural wavelength and amplitude (Levitt & Sandwell, 1995).

Figure 7 shows the free-air gravity anomalies of Jordan. The mean free-air gravity anomalies are useful in geodesy for gravity field modeling and geophysical investigations as showing average values of the Earth's density. The analysis of the free-air gravity anomalies reveals large and systematic differences in the values of the terrain roughness and mountainous areas over Jordan. Among others, gravity anomalies correlate with the elastic thickness showing the strength of the lithosphere (Watts et al., 2006). The free-air gravity anomalies of Jordan show a remarkable correlation of the values with geoid (e.g. compare Figure 7 with Figure 6) and topography of the region (compare the free-air gravity fields in Figure 7 to the DEM-based relief in Figure 12 and the topography in Figure 1). Another visible correlation and coherency between the geologic, topographic and geophysical grids are presented through the comparative analysis of Figure 7 with Figure 10 showing the aspect of the relief and Figure 9 showing slope steepness.

3.6 Hazard risk analysis by seismic data using integration of GMT and IRIS / Analiza rizika pomoću seizmičkih podataka korišćenjem integracije GMT-a i IRIS-a

The Dead Sea Fault zone is seismo-tectonically active (Abou Karaki, 1987), Figure 8. The Dead Sea Fault zone was affected by several relatively strong earthquakes with varied magnitude and focal depth, according to the IRIS database. Fig-

ure 8. Seismic events are distributed unequally along the Dead Sea Fault with most of the events concentrated around the Gulf of Aqaba. Their magnitude ranges between 2 and 6, which is recorded in seismic stations, as visualized in Figure 8. The depths of the earthquakes vary from 1 to 33 km. In contrast, local volcanoes are mostly situated in the north on the territory of present Syria.

3.7 Libraries 'raster' and 'tmap' in Rstudio / Biblioteke 'raster' i 'tmap' u RStudio paketu

Geomorphometric modeling is a technique in quantitative geomorphology used for the analysis of the fundamental Earth's surface morphology, processes, variations in the relief, and relief feature extraction by techniques of numerical modeling using the DEM. Visualized areas of high roughness and slope curvature may depict regions of certain habitats, present links with land hydrology and soil distribution. In addition, it suggests possible landslide risk hazards (computed based on slope steepness) with an increased precision due to the numerical algorithms of the DEM data processing. The improved DEM resolution and techniques of data processing by scripts presented new possibilities in Earth data analysis. In this study, four geomorphometric land-surface parameters were extracted from the DEM of Jordan by applied programming and scripting visualizing of the geospatial DEM: slope, aspect, hillshade, and elevation in Figure 9, 10, 11, and 12.

3.7.1 Slope modelling / Geomorfološko modelovanje

Figure 9 shows the slope steepness of the relief in Jordan modeled by R package 'raster' and visualized by R package 'tmap'. The input data type to geomorphometric and hydro-geomorphic relief analysis in R was the DEM, enabling modeling of relief depression, flat areas, elevations, slope steepness, and compass aspect orientation. The map includes a histogram showing the statistical behavior of data distribution.

Histogram visualization shown in the geomorphometric maps (Figure 9 to 12) is applied automatically in 'tmap' package using the `tm_lay`

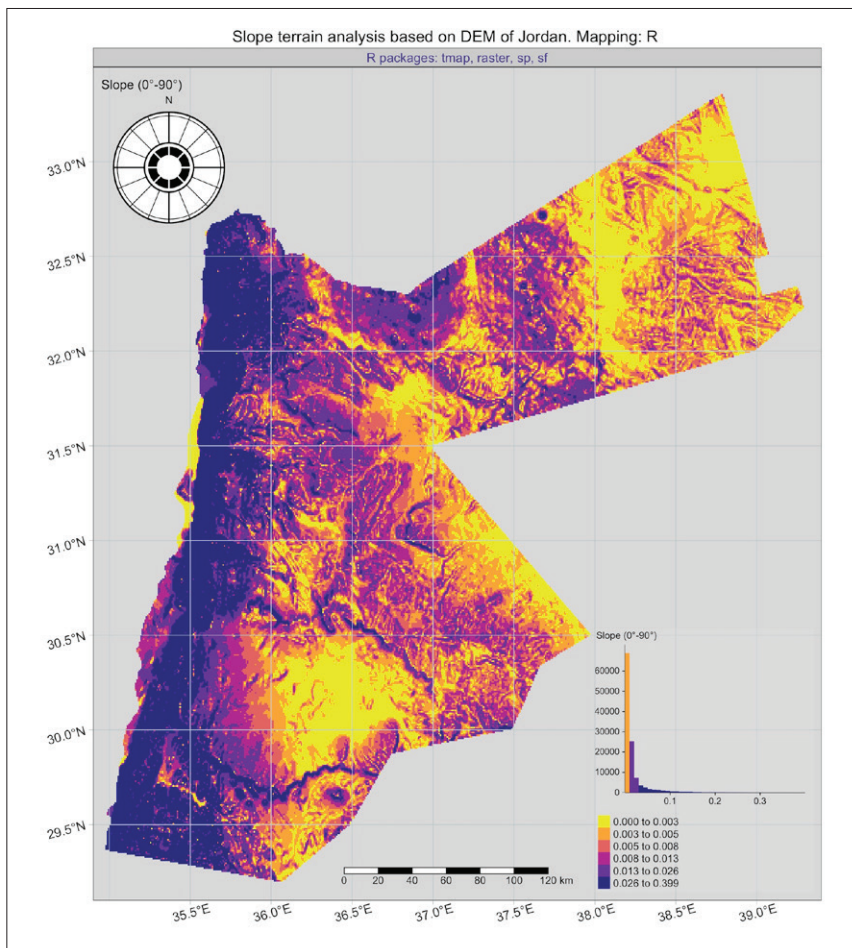


Figure 9. Slope terrain analysis based on the DEM of Jordan / *Slika 9.* Analiza terena kosina na osnovu DEM-a Jordana (Kartiranje: R)

out() function controlling legend appearance. The histogram presents an option for visual interpretation of the results illustrating data analysis by the frequency distribution of the most representative values, particularly in the areas with diverse relief such as Jordan, having both high-mountainous relief and depressions, particularly in the Dead Sea region (Salameh, 1997).

3.7.2 Aspect modelling / Modelovanje ekspozicija

The map of the relief aspect (Figure 10) shows a compass orientation of the hills and mountain ranges in Jordan with the altered display properties by the 'Spectral' color palette applied to

a displayed image (e.g. the palette, the W-E-S-N orientation and its derivatives (e.g. NE, NW, etc), displayed by color values, and additionally with a histogram showing the data distribution values. The Qa' al-Jafr depression and river network are clearly visible near the city of Ma'an (around 35,5°–37,0°E, 29,7°–30,7°N).

3.7.3 DEM hillshade and elevation modeling / DEM modelovanje nadmorskih visina

The attributes of the hillshade raster image (Figure 11) were defined using a 'tmap' functionality (palette = 'cividis', style = 'quantile', n = 10), which demonstrates the artificial illuminated light highlighting the relief of Jordan in a 3D.

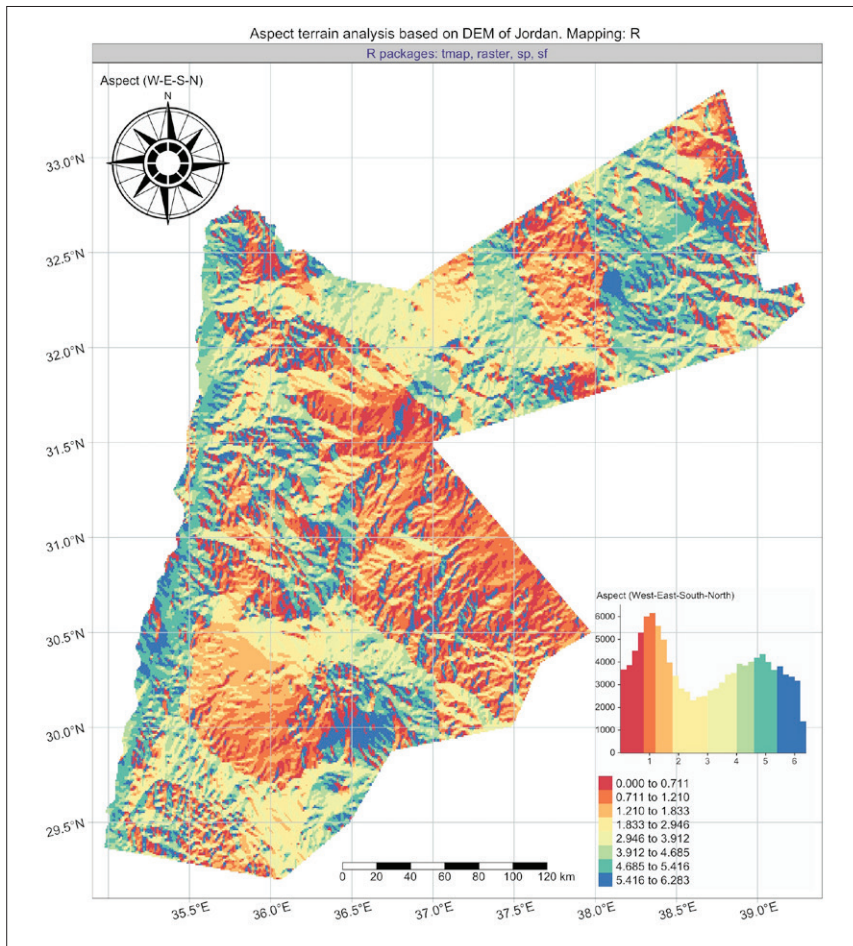


Figure 10. Aspect terrain analysis based on the DEM / *Slika 10.* Analiza ekspozicija na osnovu DEM-a (Kartiranje: R)

The DEMs have been used by R for visualization of the relief of Jordan using an embedded interpolation algorithm routine in a 'raster' package (Figure 12). The final map layout has been plotted in a 'tmap' package where the steps for the relief were set as 40 by an algorithm quan-

tile (style = 'quantile', n = 40), defined by the 'tm_raster()' function of the 'tmap' package of R. As a result (Figure 12), a raster DEM image is displayed according to z-values captured in the original tabular data by elevation.

4. DISCUSSION / DISKUSIJA

The geomorphological DEM-based data analysis is applicable for modeling groundwater and superficial hydrological streams, where topographic data provide critical input to morphometric models of water discharge, landslides, and sediment transport. In this way, it contrib-

utes to the various aspects of environmental modeling and the management of groundwater modeling of Jordan. The presented framework of the integrated data modeling and visualization by cartographic engineering is focused on the integrative cartographic visualization by

GMT, QGIS, and R for the complex data processing to generate new geospatial knowledge and data synthesis beyond separate raster and vector layers. The demonstrated analysis of the several thematic datasets (topography, seismicity,

earthquake distribution, geomorphology, tectonics, geology, and geophysics) demonstrated similar trends in data distribution in the continuous fields of the respective geospatial phenomena.

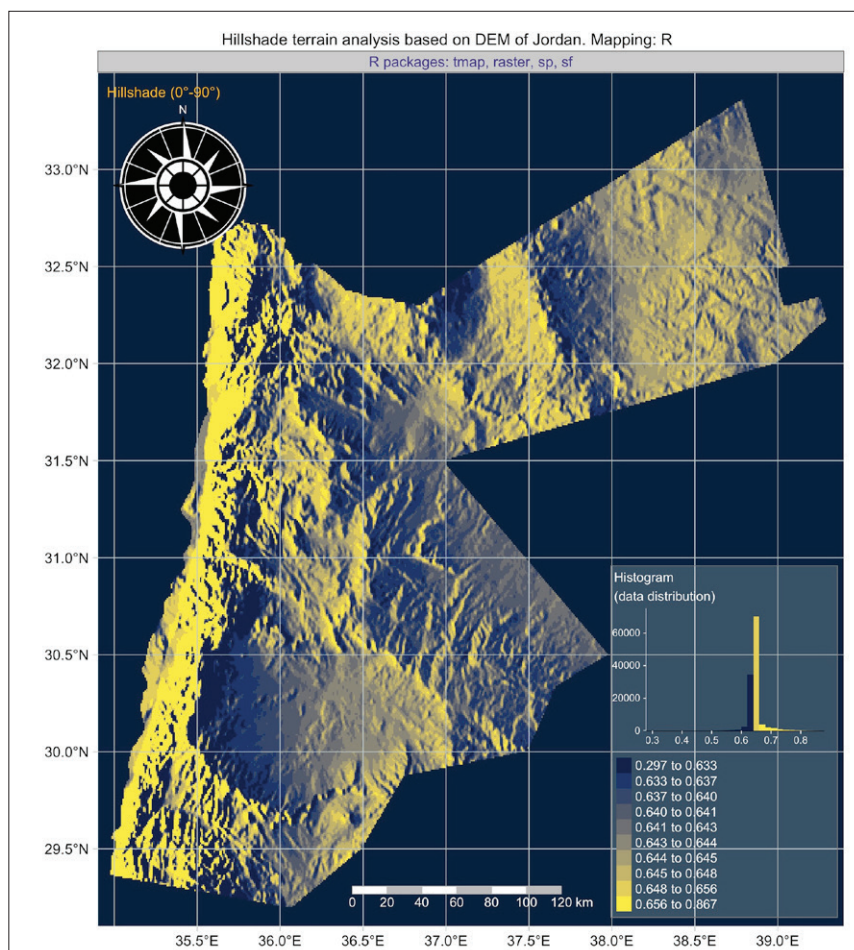


Figure 11. Hillshade visualization based on the DEM of Jordan / **Slika 11.** Vizualizacija padine zasnovan na DEM-u Jordana (Kartiranje: R)

Such approach potentially indicates the deep correlation between these phenomena using a wider approach of cartographic data processing (2D mapping, 3D modeling by GMT, QGIS, and R). Hence, the aim of the presented cartographic integration was focused on understanding the complex and still unclear nature of the Dead Sea Transform and the geomorphology of Jordan, such as the following: i) correlation between

the isolines of the relief and distribution of the geologic provinces and units, ii) correlation between the earthquakes distribution, frequency, and geophysical anomaly fields, iii) correlation between the relief slope aspect and heights.

Mountain areas, topographic depressions, river basins, and the extent of the Dead Sea Fault zone have distinct geomorphological features, consistently represented by local and regional

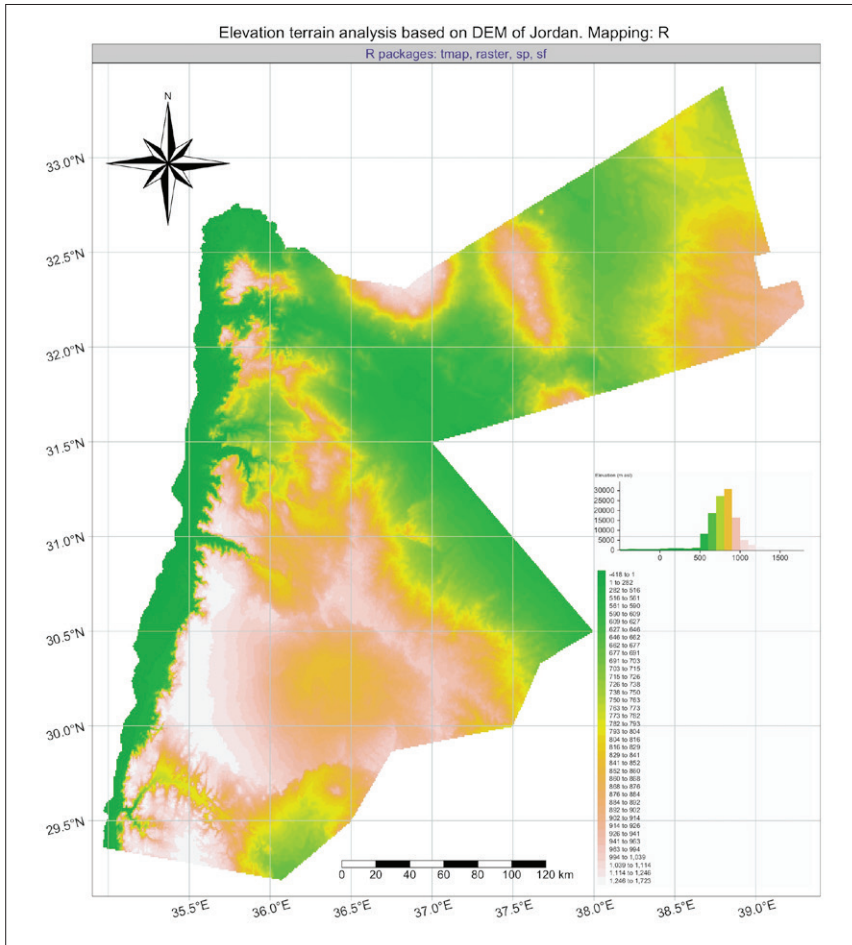


Figure 12. Relief mapping using the DEM of Jordan / *Slika 12.* Mapiranje reljefa pomoću DEM-a Jordana (Kartiranje: R)

relief, as can be compared on topographic and geomorphological maps (Figure 1 with Figures 11 and 12). Two structural aspects of the individuality in geomorphological features of Jordan include the distinctness and variability of the relief of the country and striking contrast between the major depression along the Dead Sea Fault, leveled plains in desert regions and elevations in the mountainous regions. These include, for instance, Jabal Ram, Jordanian Highlands, Abarim mountain range in the N-W, Jabal Umm ad Dami in the S as the most prominent geomorphological objects of Jordan. Their distinctness indicates the structural ambiguity of the relief boundaries and a strong correlation with the geophysical and geological setting in Jordan as discussed above.

From the engineering perspective, the research presents two cartographic outcomes: i) demonstrated integrated geoinformation approach combining scripting techniques in the mapping (GMT), programming (R) and a traditional GIS for mapping (QGIS); ii) explored geomorphology of the Dead Sea Fault zone in terms of geology, geophysics and topography in Jordan through promoting a multi-tool data processing. Thus, the research is focused on the presentation of complex data processing and visualization, including scaling, projecting and modeling, rather than technical cartographic workflow and design.

Through the presented combination of both qualitative and quantitative datasets processed by vari-

ous software tools, the methodology can be seen as complementary to the existing cartographic works with a focus on GIS (El-Naqa et al., 1999; Suetova et al., 2005; Gohl et al., 2006a, 2006b; Klaučo et al., 2013, 2017; Abou-Karaki et al., 2016; Lemenkova, 2019c). Moreover, new information on the geomorphology of Jordan is presented and produced through the coordinated cartographic process in GMT, QGIS and RStudio environments that presents a data-driven, flexible analytical mapping approach excluding the application of the predefined software. The presented methodology, compelled by data, embodies a complex workflow of raster and vector layers processing by the interchanged GIS and scripting technologies.

5. CONCLUSION / ZAKLJUČAK

Jordan is rich with a wide variety of industrial rocks presenting a stratigraphic sequence from the Precambrian basement complex to recent sediments (Khoury, 2019). Such diversity of mineral resources illustrates the value of work in geologic prognosis and exploration and explains the actuality of the cartographic approaches for the advanced and updated visualization of geology and topography of Jordan. The results include 12 new maps made by integrated data processing.

The maps illustrate datasets including the distribution of earthquakes, geophysical fields, topographic structure and geomorphologic landforms of Jordan and the Dead Sea Fault as a special area. In addition to cartographic methodology, analytical efforts presented in this manuscript focused on drivers and factors affecting the geomorphological shape of Jordan, such as geology, lithology, geophysics, topography, and tectonics with a special focus on the Dead Sea Fault as a unique region of Jordan.

Geologic evolution of the Earth's lithosphere resulting in complex processes connected to the movements of the tectonic plates (Arabian and African) present factors affecting the fundamental processes in the relief formation. Additional

By doing so, it resembles the existing use of the GMT in geomorphological, geological and geophysical datasets (Kuhn et al., 2006; Gauger et al., 2007; Lemenkova, 2020g) and integrative processing of the data connected to GIS (Al-Mahamid, 2005; Schenke & Lemenkova, 2008; Milanović et al., 2010; Alqadi & Kumar, 2013). Using multisource datasets, the research connects various raster, tabular, and vector datasets with literature analysis on the geomorphology of Jordan and considers interrelationships between the geological, tectonic, and geophysical factors as driving forces affecting the topographic shape of the country.

factors (eolian, climate, vegetation) are referred to as the external controlling processes of landform evolution having a more direct impact on local geomorphological dynamics. The focus of the study is both investigations of the geologic and tectonic setting of Jordan and engineering issues related to GIS application. Therefore, the cartographic scripting console-based methods and approaches in 2D and 3D modeling are presented as the crucial technical tools in GIS engineering applied in geological and geomorphological modeling.

By contributing to other graphical approaches, e.g. fieldwork-based GIS mapping, plotting statistical graphs, lithologic columns, visualizing flowcharts, the demand for high-quality maps in geologic and geomorphological modeling contributes not only to the data visualization but also to the increase of knowledge related to regional topography and geomorphology of Jordan. Scripting techniques of GMT and machine mapping by R language continue to technically reform the cartographic methodology along with the development of new libraries, algorithms and tools. Compared to the traditional GIS, GMT has a perspective to become more popular in mapping.

Acknowledgement / Zahvala

The author cordially thanks the anonymous reviewers and the editor for the comments and

remarks that improved the initial version of this manuscript.

References / Literatura

- Abed A.M. (1982). *Geology of Jordan*. Al Nahda Al Islamiah Library, Amman.
- Abed A.M. (2000). *Geology of Jordan*. Jordanian Geologists Association, Amman.
- Abed A.M. (2017). An overview of the geology and evolution of Wadi Mujib. *Jordan Journal of Natural History* 4: 6–28. doi:10.13140/RG.2.2.33625.98406
- Abed A.M. (2018). Geological evolution of the Azraq basin, eastern Jordan: An overview. *Jordan Journal of Natural History* 5(5): 6–52.
- Abed A.M., Yaghan R. (2000). On the paleoclimate of Jordan during the last glacial maximum. *Palaeogeography Palaeoclimatology Palaeoecology* 160: 23–33. doi:10.1016/S0031-0182(00)00042-0
- Abou Karaki N. (1987). *Synthèse et carte sismotectonique des pays de la bordure orientale de la Méditerranée: Sismicité du système de failles du Jourdain – Mer Morte*. PhD Thesis, Université Louis Pasteur de Strasbourg, Institut de Physique du Globe, 417 pp. (In French).
- Abou Karaki N., Fiaschi S., Closson D. (2016). Sustainable development and anthropogenic induced geomorphic hazards in subsiding areas. *Earth Surface Processes and Landforms* 2295: 2282–2295. doi:10.1002/esp.4047
- Abu-Allaban M., El-Naqa A., Jaber M., Hammouri N. (2015). Water scarcity impact of climate change in semi-arid regions: a case study in Mujib basin, Jordan. *Arabian Journal of Geosciences* 8: 951–959. doi:10.1007/s12517-014-1266-5
- Abu Rajab J.S., Al Tarazi E. (2018). Illuminating and optimizing a three-dimensional model of an oil shale seam and its volume distribution using the transient electromagnetic induction method, central part of Jordan. *Geophysical Prospecting* 66: 603–625. doi:10.1111/1365-2478.12547
- Al Hseinat M., Al-Rawabdeh A., Al-Zidaneen M., Ghannem H., Al-Taj M., Diabat A., Jarrar G., Atallah M. (2020). New Insights for Understanding the Structural Deformation Style of the Strike-Slip Regime along the Wadi Shueib and Amman-Hallabat Structures in Jordan Based on Remote Sensing Data Analysis. *Geosciences* 10: 253. doi:10.3390/geosciences10070253
- Al Kwatli M.A., Gillot P.Y., Lefèvre J.C., Hildenbrand A. (2015). Morpho-structural analysis of Harrat Al Sham volcanic field Arabian plate (Syria, Jordan, and Saudi Arabia): methodology and application. *Arabian Journal of Geosciences* 8: 6867–6880. doi:10.1007/s12517-014-1731-1
- Al-Laboun A.A. (1986). Stratigraphy and hydrocarbon potential of the Paleozoic succession in both Tabuk and Widyan Basins, Arabia. In: Halbouty M.T. (Ed.), *Future petroleum provinces of the world*: 399–425. doi:10.1306/M40454C14
- Al-Mahamid J. (2005). Integration of Water Resources of the Upper Aquifer in Amman-Zarqa Basin Based on Mathematical Modeling and GIS, Jordan. *Freiberg Online Geology* 12: 7–223. doi:10.23689/fidgeo-879
- Al-Sheriadeh M.S., Malkawi A.H., Al-Hamdan A., Abderahman N. (2000). Evaluating Sediment Yield at King Talal Reservoir from Landslides along Irbid-Amman Highway. *Engineering Geology* 56: 361–372. doi:10.1016/S0013-7952(99)00119-2
- Alqadi K.A., Kumar L. (2013). Are there Monthly Variations in Water Quality in the Amman, Zarqa and Balqa Regions, Jordan? *Computational Water, Energy, and Environmental Engineering* 2: 26–35. doi:10.4236/cweee.2013.22B005
- Alnawafleh H., Tarawneh K., Alrawashdeh R. (2013). Geologic and economic potentials of minerals and industrial rocks in Jordan. *Natural Science* 5(6): 756–769. doi:10.4236/ns.2013.56092
- Alsharhan A.S., Nairn A.E.M. (1997). *Sedimentary basins and petroleum geology of the Middle East*. Amsterdam, Elsevier Science B.V.: 843 pp.
- Amante C., Eakins B.W. (2009). ETOPO1 1 Arc-Minute Global Relief Model: Procedures, Data Sources and Analysis. *NOAA Technical Memorandum* 19.
- Amireh B.S., Schneider W., Abed A.M. (1994). Evolving fluvial-transitional-marine deposition through the Cambrian sequence of Jordan. *Sedimentary Geology* 89: 65–90. doi:10.1016/0037-0738(94)90084-1
- Atallah M. (1992). Tectonic evolution of northern Wadi Araba, Jordan. *Tectonophysics* 204: 17–26. doi:10.1016/0040-1951(92)90266-9

- Barbot S., Fialko Y., Sandwell D.T. (2009). Three-dimensional models of elasto-static deformation in heterogeneous media: application to the East California Shear Zone. *Geophysical Journal International* 179: 500–520. doi:10.1111/j.1365-246X.2009.04194.x
- Becker J.J., Sandwell D.T., Smith W.H.F., Braud J., Binder B., Depner J., Fabre D., Factor J., Ingalls S., Kim S-H., Ladner R., Marks K., Nelson S., Pharaoh A., Sharman G., Trimmer R., Von Rosenberg J., Wallace G., Weatherall P. (2009). Global Bathymetry and Elevation Data at 30 Arc Seconds Resolution: SRTM30_PLUS. *Marine Geodesy* 32(4): 355–371. doi:10.1080/01490410903297766
- Bender F. (1968). *Geologie von Jordanien. Biertage zur regionalen Geologie der Erde*. Geological Survey of Germany, Berlin.
- Bender F. (1974a). *Geology of Jordan*. Gebrüder Bornträger, Berlin.
- Bender F. (1974b). *Geology of the Arabian Peninsula, Jordan*. Open-File Report 74–215, 1v. (various pagings): ill., maps; 27 cm. (36 p., 2 sheets – PGS). USGS Publications Warehouse. doi:10.3133/ofr74215
- Burdon D.J. (1959). *Handbook of the geology of Jordan: To accompany and explain 1:250,000 geological map of Jordan east of the rift by A. M. Quennell*. Government of the Hashemite Kingdom, Amman.
- Choi S., Götze H.-J., Meyer U., DESIRE Group. (2011). 3-D density modelling of underground structures and spatial distribution of salt diapirism in the Dead Sea Basin. *Geophysical Journal International* 184(3): 1131–1146. doi:10.1111/j.1365-246X.2011.04939.x
- Čomić D., Anikić N. (2020). Analysis of the model for determining the economic value of mined forest areas: A case study FE Vrbanja Kotor Varoš. *Glasnik Šumarskog fakulteta Univerziteta u Banjoj Luci* 30: 45–66. doi:10.7251/GSF2030008C
- Dill H.G., Hahne K., Shaqour F. (2012). Anatomy of landslides along the Dead Sea Transform Fault System in NW Jordan. *Geomorphology* 141–142: 134–149. doi:10.1016/j.geomorph.2011.12.031
- Drăguț L., Eisank C. (2012). Automated object-based classification of topography from SRTM data. *Geomorphology* 141–142: 21–33. doi:10.1016/j.geomorph.2011.12.001
- Edgell H.S. (2006). *Arabian Deserts: Nature, Origin and Evolution*. Dordrecht, The Netherlands: Springer. doi:10.1007/1-4020-3970-0
- El-Naqa A., Hammouri N., Kuisi M. (1999). GIS-Based Evaluation of Groundwater Vulnerability in the Russeifa Area Jordan. *Revista Mexicana de Ciencias Geológicas* 23: 277–287.
- Eyal Y., Reches Z., (1983). Tectonic analysis of the Dead Sea Rift Region since the Late-Cretaceous based on mesostructures. *Tectonics* 2(2): 167–185. doi:10.1029/TC002i002p00167
- Farhan Y., Zregat D., Farhan I. (2013). Spatial Estimation of Soil Erosion Risk Using RUSLE Approach, RS, and GIS Techniques: A Case Study of Kufranja Watershed, Northern Jordan. *Journal of Water Resource and Protection* 5(12): 1247–1261. doi:10.4236/jwarp.2013.512134
- Farhan Y., Mousa R., Dagarah A., Shtaya D. (2016). Regional Hypsometric Analysis of the Jordan Rift Drainage Basins (Jordan) Using Geographic Information System. *Open Journal of Geology* 6: 1312–1343. doi:10.4236/ojg.2016.610096
- Fialko Y., Sandwell D., Simons M., Rosen P. (2005). Three-dimensional deformation caused by the Bam, Iran, earthquake and the origin of shallow slip deficit. *Nature* 435: 295–299. doi:10.1038/nature03425
- Fiaschi S., Closson D., Abou Karaki N., Pasquali P., Riccardi P., Floris M. (2017). The complex karst dynamics of the Lisan Peninsula revealed by 25 years of DInSAR observations. Dead Sea, Jordan. *ISPRS Journal of Photogrammetry and Remote Sensing* 130: 358–369. doi:10.1016/j.isprs.2017.06.008
- Foody G.M., Hill R.A. (1996). Classification of tropical forest classes from Landsat TM data. *International Journal of Remote Sensing* 17(12): 2353–2367. doi:10.1080/01431169608948777
- Fowler C.M.R. (2005). *The Solid Earth; An Introduction to Global Geophysics*. United Kingdom: Cambridge University Press: 214 pp. doi:10.1017/CBO9780511819643
- Garfunkel Z., Ben-Avraham Z. (1996). The structure of the Dead Sea basin. *Tectonophysics* 266 (1–4): 155–176. doi:10.1016/S0040-1951(96)00188-6
- Gauger S., Kuhn G., Gohl K., Feigl T., Lemenkova P., Hillenbrand C. (2007). Swath-bathymetric mapping. *Reports on Polar and Marine Research* 557: 38–45. doi:10.6084/m9.figshare.7439231
- GEBCO Compilation Group (2020). *GEBCO 2020 Grid*. doi:10.5285/a29c5465-b138-234d-e053-6c86abc040b9
- Ginat H., Enzel Y., Avni Y. (1998). Translocated Pliocene Pleistocene drainage systems along the Arava fault of the Dead Sea transform. *Tectonophysics* 284(1–2): 151–160. doi:10.1016/S0040-1951(97)00165-0

- Gohl K., Eagles G., Udintsev G., Larter R.D., Uenzelmann-Neben G., Schenke H.-W., Lemenkova P., Grobys J., Parsieglä N., Schlueter P., Deen T., Kuhn G., Hillenbrand C.-D. (2006a). Tectonic and sedimentary processes of the West Antarctic margin of the Amundsen Sea embayment and Pinelands Bay. In: *Proceeding of International Scientific Conference "2nd SCAR Open Science Meeting", 12–14 July, Hobart, Australia*. doi:10.6084/m9.figshare.7435484
- Gohl K., Uenzelmann-Neben G., Eagles G., Fahl A., Feigl T., Grobys J., Just J., Leinweber V., Lensch N., Mayr C., Parsieglä N., Rackebbrandt N., Schlüter P., Suckro S., Zimmermann K., Gauger S., Bohlmann H., Netzeband G., Lemenkova P. (2006b). Crustal and Sedimentary Structures and Geodynamic Evolution of the West Antarctic Continental Margin and Pine Island Bay. *Expedition-sprogramm* 75(XXIII/4): 11–12. doi:10.13140/RG.2.2.16473.36961
- Govedar Z., Bilić S. (2020). Application of Field-Map technology for needs of silviculture analytics in cultivated forest of Black pine in the area of Slatina. *Glasnik Šumarskog fakulteta Univerziteta u Banjoj Luci* 30: 5–20. doi:10.7251/GSF2030004G
- Halilović V., Musić J., Knežević J., Marčeta D., Drek M. (2020). Analysis of injuries at work in forestry of the Federation of Bosnia and Herzegovina – a case study PE "Unsko – sanske šume". *Glasnik Šumarskog fakulteta Univerziteta u Banjoj Luci* 30: 21–34. doi:10.7251/10.7251/GSF2030006H
- Hijmans R.J., van Etten J. (2012). *raster: Geographic analysis and modeling with raster data*. R package version 2.0-12. Retrieved May 8, 2021, from <http://CRAN.R-project.org/package=raster>
- Jarar G., Baumann A., Wachendorf H. (1983). Age determination in the Precambrian basement of the Wadi Araba Area, Southwest Jordan. *Earth and Planetary Science Letters* 63: 292–304. doi:10.1016/0012-821X(83)90043-2
- Khoury H.N. (2019). Industrial rocks and minerals of Jordan: a review. *Arabian Journal of Geosciences* 12: 619. doi:10.1007/s12517-019-4750-0
- Khrewesh A.M., Abu Hamad A., Abed A.M. (2014). Late Cretaceous Muwaqqar Formation Ammonites in Southeastern Jordan. *Jordan Journal of Earth and Environmental Sciences* 6(2): 77–83.
- Klaučo M., Gregorová B., Stankov U., Marković V., Lemenkova P. (2013). Determination of ecological significance based on geostatistical assessment: a case study from the Slovak Natura 2000 protected area. *Open Geosciences* 5(1): 28–42. doi:10.2478/s13533-012-0120-0
- Klaučo M., Gregorová B., Koleda P., Stankov U., Marković V., Lemenkova P. (2017). Land planning as a support for sustainable development based on tourism: A case study of Slovak Rural Region. *Environmental Engineering and Management Journal* 2(16): 449–458. doi:10.30638/eemj.2017.045
- Klinger Y., Avouac J.P., Abou Karaki N. (1997). Seismotectonics of Wadi Araba Fault (Jordan). European Geophysical Society 22th General Assembly Vienna-Austria. *Annales Geophysicae, Part I Society Symposia. Solid Earth Geophysics & Natural hazards* 1(15): C234.
- Klinger Y., Avouac J.P., Dorbath L., Abou Karaki N., Tisnerat N. (2000a). Seismic behaviour of the Dead Sea fault along Araba valley, Jordan. *Geophysical Journal International* 142(3): 769–782. doi:10.1046/j.1365-246x.2000.00166.x
- Klinger Y., Avouac J.P., Abou Karaki N., Dorbath L., Bourles D., Reyss J.L. (2000b). Slip rate on the Dead Sea transform fault in northern Araba valley (Jordan). *Geophysical Journal International* 142(3): 755–768. doi:10.1046/j.1365-246x.2000.00165.x
- Krienitz M.-S., Haase K.M., Mezger K., Shaikh-Mashail M.A. (2007). Magma Genesis and Mantle Dynamics at the Harrat Ash Shamah Volcanic Field (Southern Syria). *Journal of Petrology* 48(8): 1513–1542. doi:10.1093/petrology/egm028
- Kuhn G., Hass C., Kober M., Petitat M., Feigl T., Hillenbrand C.D., Kruger S., Forwick M., Gauger S., Lemenkova P. (2006). The response of quaternary climatic cycles in the South-East Pacific: Development of the opal belt and dynamics behavior of the West Antarctic ice sheet. *Expedition-sprogramm* 75(XXIII/4): 12–13. doi:10.13140/RG.2.2.11468.87687
- Lemenkov V., Lemenkova P. (2021). Using TeX Markup Language for 3D and 2D Geological Plotting. *Foundations of Computing and Decision Sciences* 46(3): 43–69. doi:10.2478/fcds-2021-0004
- Lemenkova P. (2011). *Seagrass Mapping and Monitoring Along the Coasts of Crete, Greece*. MSc. Thesis, University of Twente. doi:10.13140/RG.2.2.16945.22881
- Lemenkova P., Promper C., Glade T. (2012). Economic Assessment of Landslide Risk for the Waidhofen a.d. Ybbs Region, Alpine Foreland, Lower Austria. In: Protecting Society through Improved Understanding. In: *11th International Symposium on Landslides & the 2nd North American Symposium on Landslides & Engineered Slopes (NASL), June 2–8, 2012*. Banff, CA: 279–285. doi:10.6084/m9.figshare.7434230

- Lemenkova P. (2014). Opportunities for Classes of Geography in the High School: the Use of 'CORINE' Project Data, Satellite Images and IDRISI GIS for Geovisualization. In: *Proceedings of VII Scientific-Medotological Conference "Perspectives for the Development of Higher Education"*, Grodno, BY: 284–286. doi:10.6084/m9.figshare.7211933
- Lemenkova P. (2019a). Statistical Analysis of the Mariana Trench Geomorphology Using R Programming Language. *Geodesy and Cartography* 45(2): 57–84. doi:10.3846/gac.2019.3785
- Lemenkova P. (2019b). AWK and GNU Octave Programming Languages Integrated with Generic Mapping Tools for Geomorphological Analysis. *GeoScience Engineering* 65(4): 1–22. doi:10.35180/gse-2019-0020
- Lemenkova P. (2019c). Testing Linear Regressions by StatsModel Library of Python for Oceanological Data Interpretation. *Aquatic Sciences and Engineering* 34: 51–60. doi:10.26650/ASE2019547010
- Lemenkova P. (2019d). Automatic Data Processing for Visualising Yap and Palau Trenches by Generic Mapping Tools. *Cartographic Letters* 27(2): 72–89. doi:10.6084/m9.figshare.11544048
- Lemenkova P. (2020a), R Libraries {dendextend} and {magrittr} and Clustering Package scipy. Cluster of Python For Modeling Diagrams of Dendrogram Trees. *Carpathian Journal of Electronic and Computer Engineering* 13(1): 5–12. doi:10.2478/cjece-2020-0002
- Lemenkova P. (2020b). Applying Automatic Mapping Processing by GMT to Bathymetric and Geophysical Data: Cascadia Subduction Zone, Pacific Ocean. *Journal of Environmental Geography* 13(3–4): 15–26. doi:10.2478/jengeo-2020-0008
- Lemenkova P. (2020c). GEBCO Gridded Bathymetric Datasets for Mapping Japan Trench Geomorphology by Means of GMT Scripting Toolset. *Geodesy and Cartography* 46(3): 98–112. doi:10.3846/gac.2020.11524
- Lemenkova P. (2020d). GRASS GIS Modules for Topographic and Geophysical Analysis of the ETOPO1 DEM and Raster Data: North Fiji Basin, Pacific Ocean. *Geographia Napocensis* 14(1): 27–38. doi:10.6084/m9.figshare.13337318
- Lemenkova P. (2020e). Sentinel-2 for High Resolution Mapping of Slope-Based Vegetation Indices Using Machine Learning by SAGA GIS. *Transylvanian Review of Systematical and Ecological Research* 22(3): 17–34. doi:10.2478/trser-2020-0015
- Lemenkova P. (2020f). Python libraries matplotlib, seaborn and pandas for visualization geospatial datasets generated by QGIS. *Scientific Annals of „Alexandru Ioan Cuza” University of Iași* 64(1): 13–32. doi:10.15551/scigeo.v64i1.386
- Lemenkova P. (2020g). Geomorphology of the Puerto Rico Trench and Cayman Trough in the Context of the Geological Evolution of the Caribbean Sea. *Annales Universitatis Mariae Curie-Skłodowska, sectio B – Geographia, Geologia, Mineralogia et Petrographia* 75: 115–141. doi:10.17951/b.2020.75.115-141
- Lemenkova P. (2021). Exploring structured scripting cartographic technique of GMT for ocean seafloor modeling: A case of the East Indian Ocean. *Maritime Technology and Research* 3(2): 162–184. doi:10.33175/mtr.2021.248158
- Levitt D.A., Sandwell D.T. (1995). Lithospheric bending at subduction zones based on depth soundings and satellite gravity. *Journal of Geophysical Research* 100: 379–400. doi:10.1029/94JB02468
- Löhrer R., Bertrams M., Eckmeier E., Protze J., Lehmkuhl F. (2013). Mapping the distribution of weathered Pleistocene wadi deposits in Southern Jordan using ASTER, SPOT-5 data and laboratory spectroscopic analysis. *CATENA* 107: 57–70. doi:10.1016/j.catena.2013.02.003
- Marder E., Bookman R., Filin S. (2018). Geomorphological response of the Lower Jordan River basin to active tectonics of the Dead Sea Transform. *Geomorphology* 317: 75–90. doi:10.1016/j.geomorph.2018.05.018
- Marks K.M., Sandwell D.T. (1991). Analysis of Geoid Height versus Topography for Oceanic Plateaus and Swells using Nonbiased Linear Regression. *Journal of Geophysical Research* 96: 8045–8055. doi:10.1029/91JB00240
- Milanović Đ., Stupar V., Brujić J., Nikić D. (2010). Distribution of autochthonous dendro-species in the Management Unit „Ozren“-Petrovo – implementation of GIS technology. *Glasnik Šumarskog fakulteta Univerziteta u Banjoj Luci* 13: 1–17.
- Miletić M., Milanović Đ., Stupar V., Brujić J. (2016). Forest vegetation of Trešnjik near Banja Luka. *Glasnik Šumarskog fakulteta Univerziteta u Banjoj Luci* 25: 15–40. doi:10.7251/GSF1625015M
- Obeidat M.M., Awawdeh M., Abu Al-Rub F. (2013). Multivariate statistical analysis and environmental isotopes of Amman/Wadi Sir (B2/A7) groundwater, Yarmouk River Basin, Jordan. *Hydrological Processes* 27: 2449–2461. doi:10.1002/hyp.9245
- Obeidat M., Awawdeh M., Al-Kharabsheh N., Al-Ajlouni A. (2021). Source identification of nitrate in the upper aquifer system of the Wadi Shueib catchment area in Jordan based on stable isotope

- composition. *Journal of Arid Land* 13: 350–374. doi:10.1007/s40333-021-0055-8
- Oruç B., Pamukçu O., Sayın T. (2019). Isostatic Moho undulations and estimated elastic thicknesses of the lithosphere in the central Anatolian plateau, Turkey. *Journal of Asian Earth Sciences* 170: 166–173. doi:10.1016/j.jseaes.2018.11.001
- Pavlis N.K., Holmes S.A., Kenyon S.C., Factor J.K. (2012). The development and evaluation of the Earth Gravitational Model 2008 (EGM2008). *Journal of Geophysical Research* 117: B04406.
- Pollastro R.M., Karshbaum A.S., Viger R.J. (1999). *Maps showing geology, oil and gas fields and geologic provinces of the Arabian Peninsula*. U.S. Geological Survey Open-File Report 97-470-B: 14.
- QGIS.org (2020). *QGIS Geographic Information System*. QGIS Association. <http://www.qgis.org>
- Quennell A.M. (1951). The geology and mineral resources of (former) Trans-Jordan. *Colonial geology and mineral resources* 2(2): 85–115.
- Petković V., Marčeta D., Španjić S., Kosović M. (2015). Determination of skidding distance with GIS in the lowland and hilly terrain conditions. *Glasnik Šumarskog fakulteta Univerziteta u Banjoj Luci* 23: 5–14. doi:10.7251/GSF1523005P
- R Core Team (2020). *R: A language and environment for statistical computing*. Foundation for Statistical Computing, Vienna, Austria. <https://www.R-project.org/>
- RStudio Team (2017). *RStudio: Integrated Development Environment for R*. RStudio, Inc., Boston, MA. <https://www.RStudio.com/>
- Riad P., Graefe S., Hussein H., Buerkert A. (2020). Landscape transformation processes in two large and two small cities in Egypt and Jordan over the last five decades using remote sensing data. *Landscape and Urban Planning* 197: 103766. doi:10.1016/j.landurbplan.2020.103766
- Sadooni F.N., Dalqamouni A. (1998). Geology and petroleum prospects of Upper Triassic sediments, Jordan. *Marine and Petroleum Geology* 15(8): 783–801. doi:10.1016/S0264-8172(98)00046-4
- Salameh H.R. (1997). Geomorphology of the eastern coast of the Dead Sea. *GeoJournal* 41(3): 255–266. doi:10.1023/A:1006826029306
- Salvador R., Pons X. (1998). On the applicability of Landsat TM images to Mediterranean forest inventories. *Forest Ecology and Management* 104(1–3): 193–208. doi:10.1016/S0378-1127(97)00264-8
- Sandwell D., Schubert G. (1980). Geoid height versus age for symmetric spreading ridges. *Journal of Geophysical Research* 85(B12): 7235–7241. doi:10.1029/JB085iB12p07235
- Sandwell D.T., McAdoo D.C. (1990). High Accuracy, High Resolution Gravity Profiles from 2 Years of Geosat Exact Repeat Mission. *Journal of Geophysical Research* 95: 3049–3060. doi:10.1029/JC095iC03p03049
- Sandwell D., Garcia E., Soofi K., Wessel P., Chandler M., Smith W.H.F. (2013). Toward 1-mGal accuracy in global marine gravity from CryoSat-2, Envisat, and Jason-1. *The Leading Edge* 32(8): 892–899. doi:10.1190/tle32080892.1
- Sandwell D.T., Müller R.D., Smith W.H.F., Garcia E., Francis R. (2014). New global marine gravity model from CryoSat-2 and Jason-1 reveals buried tectonic structure. *Science* 346(6205): 65–67.
- Schenke H. (2016). General Bathymetric Chart of the Oceans (GEBCO). In: Harff J., Meschede M., Petersen S., Thiede J. (Eds.), *Encyclopedia of Marine Geosciences; Encyclopedia of Earth Sciences Series*. Springer, Dordrecht. doi:10.1007/978-94-007-6238-1_63
- Schenke H.W., Lemenkova P. (2008). Zur Frage der Meeresboden-Kartographie: Die Nutzung von AutoTrace Digitizer für die Vektorisierung der Bathymetrischen Daten in der Petschora-See. *Hydrographische Nachrichten* 81: 16–21. doi:10.6084/m9.figshare.7435538
- Sideris M.G. (2011). Geoid, Computational Method. In: Gupta H.K. (Eds.), *Encyclopedia of Solid Earth Geophysics; Encyclopedia of Earth Sciences Series*. Springer, Dordrecht. doi:10.1007/978-90-481-8702-7_225
- Smit J., Brun J.-P., Cloetingh S., Ben-Avraham Z. (2010). The rift-like structure and asymmetry of the Dead Sea Fault. *Earth and Planetary Science Letters* 290(1–2): 74–82. doi:10.1016/j.epsl.2009.11.060
- Smith B., Sandwell D. (2003). Accuracy and Resolution of Shuttle Radar Topography Mission Data. *Geophysical Research Letters* 30(9): 1467. doi:10.1029/2002GL016643
- Stupar V., Milanović Đ. (2017). History of nature protection in the Sutjeska National Park. *Glasnik Šumarskog fakulteta Univerziteta u Banjoj Luci* 26: 113–128. doi:10.7251/GSF17261135
- Suetova I.A., Ushakova L.A., Lemenkova P. (2005). Geoinformation mapping of the Barents and Pechora Seas. *Geography and Natural Resources* 4: 138–142. doi:10.6084/m9.figshare.7435535
- Tozer B, Sandwell D.T., Smith W.H.F., Olson C., Beale J.R., Wessel P. (2019). Global bathymetry and topography at 15 arc sec: SRTM15+

- Earth and Space Science* 6: 1847–1864. doi:10.1029/2019EA000658
- Valjarević A., Djekić T., Stevanović V., Ivanović R., Jandžiković B. (2018a). GIS numerical and remote sensing analyses of forest changes in the Toplica region for the period of 1953–2013. *Applied Geography* 92: 131–139. doi:10.1016/j.apgeog.2018.01.016
- Valjarević A., Srećković-Batočanin D., Valjarević D., Matović V. (2018b). A GIS-based method for analysis of a better utilization of thermal-mineral springs in the municipality of Kursumlija (Serbia). *Renewable and Sustainable Energy Reviews* 92: 948–957. doi:10.1016/j.rser.2018.05.005
- Watts A.B., Sandwell D.T., Smith W.H.F., Wessel P. (2006). Global gravity, bathymetry, and the distribution of submarine volcanism through space and time. *Journal of Geophysical Research* 111: B08408. doi:10.1029/2005jb004083
- Wessel P., Luis J.F., Uieda L., Scharroo R., Wobbe F., Smith W.H.F., Tian D. (2019). The Generic Mapping Tools version 6. *Geochemistry, Geophysics, Geosystems* 20: 5556–5564.

Sažetak

U ovom istraživanju razvijen je integrisani okvir za analizu podataka o Zemlji (“Big Earth data”) u kontekstu geomorfologije Jordana. Istraživanje se bavi korelacijom između nekoliko tematskih skupova podataka, uključujući mašinsko učenje i multidisciplinarnu geoprostorne podatke. GIS kartiranje se široko koristi u geološkom mapiranju kao najadekvatnije tehničko sredstvo za vizualizaciju i analizu podataka. GIS aplikacije podstiču geološko prospektivno modeliranje vizualizacijom podataka usmjerenih na prognozu mineralnih resursa. Međutim, automatizacija pomoću mašinskog učenja za obradu velikih podataka o Zemlji pruža brzinu i tačnu obradu masivnih skupova podataka iz više izvora. To je moguće primjenom skriptiranja i programiranja u kartografskim tehnikama. Ova studija predstavlja kombinovane metode mašinskog učenja kartografske analize i modeliranja velikih podataka o Zemlji. Cilj studije je da se analizira povezanost faktora koji utiču na geomorfološki oblik Jordana u odnosu na rasjed Mrtvog mora i geološku evoluciju. Tehnička metodologija uključuje tri nezavisna alata: 1) Generic Mapping Tools (GMT); 2) odabrane biblioteke programskog jezika R; 3) QGIS. Konkretno, GMT skriptni program korišćen je za topografsko, seizmičko i geofizičko mapiranje; QGIS - za geološko mapiranje; Programski jezik R - za geomorfometrijsko modeliranje. Shodno tome, tok rada je logično strukturisan kroz ova tri tehnička alata, predstavljajući različite kartografske pristupe za obradu podataka. Podaci i materijali uključuju skupove podataka iz više izvora različite rezolucije, prostornog opsega, porijekla i formata. Rezultati su predstavili kartografske rasporede kvalitativnih i kvantitativnih karata sa statističkim rezimeom (histogrami). Novost ovog pristupa objašnjava se potrebom da se smanji tehnički jaz između tradicionalnog GIS-a i skripti za kartiranje, koje je bitno za mapiranje velikih podataka, gdje su presudni faktori brzina i preciznost rukovanja podacima i efikasna vizuelizacija postignuta mašinskom grafikom. U radu se analiziraju osnovni geološki procesi koji utiču na formiranje geomorfoloških oblika terena u Jordanu sa 3D vizualizacijom izabranog fragmenta zone rasjeda Mrtvog mora. Istraživanje predstavlja prošireni opis metodologije, uključujući objašnjenja isječaka koda iz modula GMT i primjere upotrebe R-biblioteka *,raster’* i *,tmap’*. Rezultati su otkrili snažnu korelaciju između geoloških i geofizičkih karakteristika terena i geomorfoloških obrazaca. Integrisano proučavanje geomorfologije Jordana zasnovano je na skupovima podataka koji obrađuju više scenarija. Temeljnou analizom predstavljene su regionalne korelacije između geomorfološkog, geološkog i tektonskog okruženja u Jordanu. Rad je doprinio razvoju kartografskog inženjerstva uvođenjem skriptnih tehnika i regionalnim studijama Jordana, uključujući Mrtvo more kao posebnu regiju Jordana. Rezultati uključuju 12 novih tematskih mapa, uključujući 3D model.

Ključne reči: geofizika, geologija, GMT, Jordan, kartografija, mašinsko učenje, Mrtvo more, QGIS, topografija, veliki podaci